Chem Biol Drug Des 2012; **79:** 194–201

Research Article

doi: 10.1111/j.1747-0285.2011.01271.x

Anticancer Activity of an Imageable Curcuminoid 1-[2-Aminoethyl-(6-hydrazinopyridine-3-carbamidyl)-3,5-bis-(2-fluorobenzylidene)-4-piperidone (EFAH)

Pallavi Lagisetty, Dharmalingam Subramaniam, Kaustuv Sahoo, Shrikant Anant and Vibhudutta Awasthi*

Department of Pharmaceutical Sciences and Small Animal Imaging Facility, University of Oklahoma Health Science Center, 1110 N, Stonewall Avenue, Oklahoma City, OK 73117, USA
**Corresponding author: Vibhudutta Awasthi, vawasthi@ouhsc.edu*

3,5-Bis(2-fluorobenzylidine)-4-piperidone or EF24 is a potent anticancer derivative of curcumin. Using an amine derivative of EF24, we synthesized a hydrazinonicotinic acid conjugate, EFAH, for Tc-99m radiolabelling and single photon emission tomography imaging. The aqueous solubility of EFAH (3.5 mg/mL) was significantly more than that of EF24 (1.2 mg/mL); the octanol/water partition coefficient of EFAH was estimated at log P = 0.33. As an antiproliferative agent, EFAH was as effective as EF24 in suppressing the proliferation of H441, MiaPaCa-2 and Panc-1 cells. Daily intraperitoneal injection of EFAH (5 μg) for 3 weeks in mice carrying xenografts of Panc-1 pancreatic cancer showed a mean tumour volume reduction of 79%; the tumour weight decreased by 82% in the treated group. For imaging and biodistribution, EFAH was labelled with Tc-99m (98% RCY) and intravenously administered in rats. Approximately 23.7% and 14.3% of injected dose accumulated in liver and intestine, respectively, suggesting that EFAH is mostly eliminated by hepatobiliary route. The results indicate that HYNIC modification of EF24 for Tc-99m radiolabelling does not affect its antiproliferative efficacy. For the first time, a visual biodisposition of EF24 in a live animal model has been demonstrated. Such knowledge could be of benefit in developing therapeutic curcuminoids, such as EF24.

Key words: cancer, curcuminoid, EF24, imaging, single photon emission tomography, Tc-99m

Received 24 May 2011, revised 21 September 2011 and accepted for publication 16 November 2011

There is a growing understanding among cancer researchers about the utility of visual, temporal and quantitative information pertaining to the delivery of drug in tumour tissue. In most instances, imaging can provide such enabling technologies where the ability to image the distribution of drug may offer an important tool in real-time management of therapy. Molecularly targeted drugs are especially amenable to this strategy. Arguably, as drug distribution may be heterogeneous even in histologically identical tumours, image-based knowledge of drug accumulation in cancer tissue may help in predicating the drug effect. The focus in our laboratory has been to add imaging dimension to the development of anticancer drugs by synthesizing related compounds that could be easily monitored by non-invasive imaging. The role of such technology in hastening anticancer drug development is acknowledged in a Critical Path Initiative by the FDA and NCI (1–3). Imaging provides both structural and functional information under physiologic conditions and eliminates the sampling errors inherent in other methods (4). It is also possible to carry out longitudinal studies in the same subject to collect time-point-specific data. We describe results of our study on the development of a novel imageable curcuminoid.

Curcumin is an unsaturated polyphenolic β-ketone present in the rhizome of Indian dietary spice turmeric (*Curcuma longa* L.). Several investigations have demonstrated that curcumin is chemopreventive in all three stages of carcinogenesis – initiation, progression and promotion (5–9). The pharmacological safety and efficacy of curcumin make it an attractive therapeutic molecule, but the poor bioavailability after oral administration remains a major barrier (10). The problem of bioavailability has been attributed to its lack of water solubility, inefficient absorption and rapid metabolism (11). It is therefore of interest to modify the core structure of curcumin with a goal of enhanced bioavailability and potency. Synthetic analogues of curcumin with enhanced cytotoxicity and improved physicochemical properties are now emerging (12–14). One of these compounds is 3,5-bis(2-fluorobenzylidine)-4-piperidone (also known as EF24) which has been shown to possess potent anticancer activity, both *in vitro* and *in vivo* (15).

In this study, we report the synthesis of a modified EF24 derivative, 1-[2-aminoethyl-(6-hydrazinopyridine-3-carbamidyl)-3,5-bis-(2-fluorobenzylidene)-4-piperidone (EFAH). EFAH could be efficiently labelled with a gamma ray-emitting Tc-99m radionuclide. We demonstrate that the modification does not affect the antiproliferative activity of 3,5-bis(benzylidene)-4-piperidone series in cancer cells, both *in vitro* and *in vivo*. Finally, we show that the Tc-99m-labelled analogue of the compound provides quantitative information about biodistribution from single photon emission tomography (SPECT) in a rat

model. To our knowledge, this is the first image-based non-invasive investigation of EF24.

Methods and Materials

All reagents were obtained from commercial sources and were used directly without further purification. ^{1}H NMR spectra and ^{13}C NMR spectra were recorded at 300 and 75 MHz on Varian VX-300 (Varian Inc., Palo Alto, CA, USA). The spectra were referenced to the residual protonated solvents. Abbreviations such as *s*, *d*, *t*, *m*, *br* and *dd* used in the description of NMR spectra denote *singlet*, *doublet*, *triplet*, *multiplet*, *broad*, and *double doublet* respectively. The chemical shifts and coupling constants were reported in δ parts per million (p.p.m.) and hertz (Hz), respectively. The mass spectra were recorded by Finnigon MAT LCQ mass spectrometer (San Jose, CA, USA). The NMR and mass spectroscopy data for the synthesized compounds are provided in the supplemental document (Appendix S1). The reverse-phase high-performance liquid chromatography (RP-HPLC) was performed with Beckman Model 126 pump, 166 absorbance detector, Bioscan Model B-FC-300 radioisotope detector. HPLC solvents consisted of water and acetonitrile with 0.1% trifluoroacetic acid. Radionuclide Tc-99m, as pertechnetate, was obtained from OUHSC Nuclear Pharmacy (Oklahoma City, OK, USA). All intermediate and final products were monitored by thin layer chromatography (TLC) on 250-μm silica plates. Where applicable, the compounds were purified by column chromatography using 200–300 mesh silica gel columns. Melting points were recorded on an Electrothermal Mel-Temp melting point apparatus (Thermo Scientific, Waltham, MA, USA). The reported melting points (°C) are uncorrected.

3,5-Bis-(2-fluorobenzylidene)-4-piperidone (1)

Hydrochloric Acid gas (generated *in situ*) was bubbled into a solution of 4-piperidone hydrochloride monohydrate (3 g, 19.5 mmol) in glacial acetic acid (80 mL) until a clear solution was obtained (about 15 min). To the reaction mixture, 2-fluorobenzaldehyde (6 mL, 56.5 mmol) was added and the mixture was left at room temperature for 48 h. The crystals formed were filtered on a Buchner funnel, washed with absolute ethanol (50 mL) and ether (50 mL), and followed by drying to obtain **1** as yellow crystalline solid (5.71 g, 94% yield, m.p. 185–186 °C). Free base of **1** was generated by treating the acetate salt with 10% potassium carbonate solution.

1-(2-Aminoethyl)-3,5-bis-(2-fluorobenzylidene)-4-piperidone (2)

2-Bromoethylamine hydrobromide (204 mg, 1.00 mmol), compound **1** (311 mg, 1.00 mmol), cesium carbonate (325 mg, 1.00 mmol) and potassium iodide (166 mg, 1.00 mmol) were taken together in a flask containing DMF (5 mL). The reaction mixture was heated at 80 °C for 18 h. The progress of the reaction was monitored by an appearance of a new spot in silica TLC. After the reaction was complete, the reaction mixture was filtered and the solvent was dried. The residue was dissolved in chloroform and washed with saturated sodium chloride solution followed by water. The organic phase was separated, dried over anhydrous sodium sulphate and concentrated to obtain a crude yellow solid. The crude compound was passed through a silica column, and the title compound was eluted with 10% methanol in methylene chloride. The fractions containing the pure compound were collected and concentrated to dryness to obtain the compound **2** as a yellow solid (252 mg, 53% yield, m.p. 151–152 °C).

N′-(5-{2-[3,5-Bis-(2-fluorobenzylidene)-4-oxo-piperidin-1-yl]-ethylcarbamoyl}-pyridin-2-yl)-hydrazinecarboxylic acid tert-butyl ester (3)

Succunimidyl-6-*boc*-hydrazinonicotinic acid was synthesized in-house following a reported method (16). Succunimidyl-6-*boc*-hydrazinonicotinic acid (360 mg, 1.03 mmol) was added to compound **2** (280 mg, 0.79 mmol) in DMF containing diisopropyl ethylamine (650 μL, 3.95 mmol). The reaction mixture was stirred at room temperature for 48 h and monitored by TLC where a new spot appeared with polarity in between the reactants. After completion of the reaction, the solvent was evaporated to dryness, and the pure conjugate was separated by column chromatography on silica (200–300 mesh) with 10% methanol in chloroform. The fractions containing the desired compound were collected and dried to yield compound **3** as yellow foamy solid (290 mg, 62% yield, m.p. 123–125 °C). R_f (10% methanol in chloroform) = 0.40.

N-{2-[3,5-Bis-(2-fluorobenzylidene)-4-oxo-piperidin-1-yl]-ethyl}-6-hydrazinonicotinamide (4)

To deprotect compound **3**, hydrochloric acid (55 μL of 11 N) was added to a solution of compound **3** in 5 mL of methylene chloride (120 mg, 0.20 mmol). The reaction mixture was stirred at room temperature for 5 h, and a slower moving spot was obtained in TLC. The reaction mixture was evaporated to dryness, and compound **4** was isolated as yellow solid. Methylene chloride and ether wash was given to the solid to remove the impurities (86 mg, 87% yield, m.p. 222–224°C). R_f (30% MeOH in Chloroform) = 0.10.

Partition coefficient

The partition coefficient ($K_{O/W}$) was determined in triplicate in octanol/water system. The initial oil and water phases were prepared as phases saturated in the other solvent. About 20 mL of octanol was mixed with 20 mL deionized water in a screw-capped glass bottle and agitated overnight at 25 °C. The mixture was allowed to settle for 6 h to separate water-rich octanol phase (oil phase), from octanol-rich water phase (water phase). About 3.0 mg of drug was dissolved in 2 mL of oil phase in a screw-capped glass tube, and 2 mL of water phase was added. The tubes were agitated overnight followed by a 6 h equilibrium period. EFAH was spectrophotometrically analysed in both the phases and estimated against a calibration curve. $K_{O/W}$ was calculated as a ratio between drug in oil and water phases.

Tc-99m-labelled N*-{2-[3,5-Bis-(2-fluorobenzylidene)-4-oxo-piperidin-1-yl]-ethyl}-6-hydrazinonicotinamide (5)*

About 300 μL of tricine solution (100 mg/mL in water) was added to a solution of compound **4** (30 μg) in 30 μL water. $Na^{99m}TcO_4$ (2 mCi in 0.5 mL of saline) and 10 μL $SnCl_2$ solution (1 mg/mL in

1 N HCl) were added to the reaction mixture. The reaction mixture was incubated at room temperature for 15 min. Quantitative radiolabelling (>95%) was obtained within 15 min of incubation at room temperature. The labelling was followed by Whatman paper chromatography in acetone where free pertechnetate had an R_f of 0.8 and the labelled compound had an R_f of 0.1. Upon radio-RP-HPLC using a gradient of acetonitrile (20–100%) at 1.5 mL/min at 254 nm, compound **5** eluted at 9.2 min without any contamination of free pertechnetate (2.5 min).

Stability of Tc-99m label against plasma challenge

The stability of Tc-99m labelling of EFAH was tested by challenging Tc-99m-EFAH with plasma at 37 °C for up to 24 h. Briefly, about 300 μL of human plasma was incubated with 148 MBq (200 μL) of Tc-99m-EFAH. After indicated times, a 10-μL aliquot of supernatant was injected into a reverse-phase HPLC column (C-18, 10 μm Sonoma) eluted under a 20-min gradient of acetonitrile (20–100%) at 1.5 mL/min.

Cell culture and drug treatment

Human lung adenocarcinoma cell line NCI-H441 (ATCC Number: HTB-174) was obtained from the American Type Culture Collection (Manassas, VA, USA). H441 cells were maintained at 37 °C with 5% CO_2 in McCoy's 5A Medium (Invitrogen, Carlsbad, CA, USA) supplemented with 5% heat-inactivated foetal bovine serum (FBS) and gentamicin (Gibco Laboratories, Grand Island, NY, USA). Pancreatic cancer cells Panc-1 and MiaPaCa-2 were maintained in RPMI 1640 1× (Catalogue number 11 875) in 10% heat-inactivated FBS; penicillin at 100 U and streptomycin at 100 μg/mL of medium were added as antibiotics.

To evaluate the antiproliferative activity of synthesized compounds, the cells were seeded in a 96-well flat bottom tissue culture plates at a density of 5×10^3 cells per well. The cells were allowed to attach and grow overnight. The test compounds were dissolved in dimethyl sulfoxide (DMSO) and added to cells in the culture medium supplemented with 5% FBS. The DMSO concentration was maintained at 0.1% per well. The control wells received equivalent volume of DMSO without any drugs. The cells were allowed to remain in the treatment medium for 24, 48 and 72 h.

Cell proliferation

The total number of cells after treatment was estimated by hexosaminidase assay (17). Briefly, the medium was removed and hexosaminidase substrate solution in citrate buffer pH 5 (7.5 mM), *p*-nitrophenol-*N*-acetyl-beta-D-glucosaminidase (Calbiochem, San Diego, CA, USA), was added at 60 μL per well. The plate was incubated at 37 °C in 100% humidity for 30 min, before stopping the reaction by adding 90 μL of 50 mM glycine containing 5 mM of EDTA (pH 10.4); absorbance was measured at 405 nm.

Animal studies

The animal experiments were performed according to the NIH Animal Use and Care Guidelines and were approved by the Institutional Animal Care Committee of the University of Oklahoma Health Sciences Center.

Biodistribution of Tc-99m-EFAH

Female athymic nude rats (125–150 g) were obtained from Harlan Laboratories (Indianapolis, IN, USA), and housed in a controlled environment with 12 h day/night cycle. The animals were allowed to acclimatize at least 1 week before inoculation of lung adenocarcinoma H441 cells. On the day of tumour implantation, the animals were anaesthetized with 2–3% isoflurane in oxygen stream. About 0.1 mL H441 cell suspension in phosphate-buffered saline (100 million cells/mL) was subcutaneously injected in the left dorsal thigh region. The animals were returned to their cages, and the tumour was allowed to grow till a palpable tumour was visible in majority of the animals.

We investigated the distribution of Tc-99m-EFAH by imaging in a NanoSPECT machine (Bioscan, Washington, DC, USA). The rats were anaesthetized using 2–3% isoflurane in oxygen stream and placed inside the detector. The body temperature was maintained at 37 ± 1 °C by Minerve anaesthesia system (Bioscan). Approximately 500 μCi of Tc-99m-EFAH (~0.2 mL) was intravenously injected in the tail vein. Planar whole-body images were acquired at various times over 24 h. After the final imaging session at 24 h, the rats were subjected to a biodistribution study. Briefly, the animals were euthanized by an intraperitoneal overdose of a euthanasia solution (Euthasol, Virbac Corporation, Fort Worth, TX, USA). Various organs were excised, washed with saline, weighed, and appropriate tissue samples were counted in an automated gamma counter (Perkin-Elmer, Boston, MA, USA). Total blood volume, bone and muscle mass were estimated as 5.7%, 10% and 40% of body weight, respectively. A diluted sample of injected Tc-99-EFAH served as a standard for comparison.

Mouse model of xenograft tumour

Panc-1 cells (ATCC) were grown in RPMI 1640, containing 10% heat-inactivated foetal bovine serum (Sigma Chemical Co., St. Louis, MO, USA) and 1% antibiotic–antimycotic solution (Mediatech, Inc.) at 37 °C in a humidified atmosphere of 5% CO_2. Five-week-old male athymic nude mice (The Jackson Laboratory, Bar Harbor, ME, USA) were maintained with water and standard mouse chow *ad libidum*. The animals were injected with 1×10^6 cells in the left and right flank and allowed to form xenografts. EFAH was intraperitoneally administered daily (5 μg/injection) for 3 weeks until killing. Tumours were measured weekly with a Vernier caliper, and the tumour volumes were calculated according to the formula length × width × depth × 0.5236. At the end of the treatment, the animals were killed, and the tumours were removed and weighed.

Data analysis

The *in vitro* biological data were analysed for significance of difference at $p < 0.05$ using PRISM 5.0 (GraphPad Software, Inc., La Jolla, CA, USA). The *in vivo* biodistribution data were analysed for presentation as per cent injected dose per gram tissue as well as

accumulation per organ. All data were corrected for the decay of Tc-99m radioactivity (physical decay $T_{1/2}$ = 6 h).

Results and Discussion

Despite recent advances in molecular and tumour biology in cancer and the introduction of several new agents, inclusive of molecularly targeted therapies, the disease continues to be a contemporary challenge. Chemotherapy with anticancer drugs is the mainstay for the treatment of cancer. Antineoplastic agents are cytotoxic by design and can cause severe systemic adverse effects in therapeutic doses. Curcumin and its synthetic analogues have shown some selectivity towards cancer cells. For instance, it has been shown that curcumin is antiproliferative in cancerous cells without being toxic to normal cells (18). We also showed recently that a congener of curcuminoid EF24 is not toxic to lung fibroblasts, but suppresses growth of cancer cells (19,20). To enable labelling of EF24 with imageable radionuclide, we modified 3,5-bis-(2-fluorobenzylidene)-4-piperidone to carry HYNIC moiety and investigated whether the intrinsic anticancer activity of the compound is preserved after the modification. The synthesis of EF24 was accomplished by acid-catalysed Claisen-Schmidt condensation of 4-piperidone and 2-fluoro benzaldehyde, and has been reported elsewhere (21,22).

Synthesis and Tc-99m radiolabelling

In our previous studies, we have shown that modification of piperidinyl nitrogen in EF24 does not adversely affect its activity (23). Here, we modified piperidinyl nitrogen with bromoethylamine to obtain compound **2** (82% yield). Upon a reaction of *N*-hydroxysuccinimidyl-6-*boc*-hydrazino nicotinamide with the free primary amine in **2,** compound **3** containing a hydrazinonicotinoyl (HYNIC) moiety was obtained, which on deprotection afforded compound **4** (Figure 1). Compared to the precursor EF24, EFAH

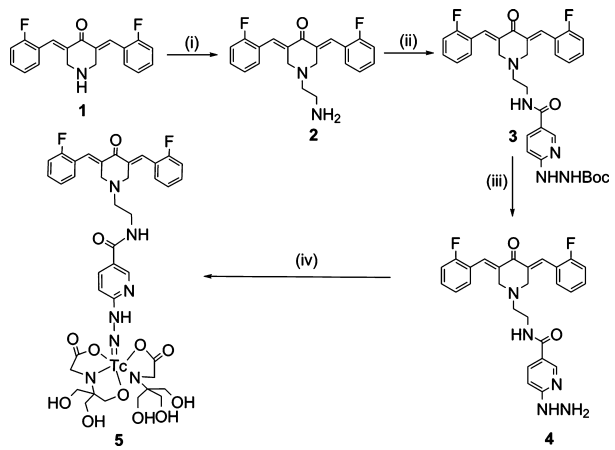

Figure 1: Synthesis of EFAH. The reactions conditions were as follows: (i) bromoethylamine, KI, Cs_2CO_3, DMF, 80 °C, 5 h; (ii) HYNIC, DMF, DIPEA, room temperature, 24 h; (iii) DCM, HCl, room temperature, 2 h, and (iv) tricine, $Na^{99m}TcO_4$, Stannous chloride, room temperature, 15 min.

was found to possess more aqueous solubility (1.2 versus 3.5 mg/mL, respectively). This may be of significance in the design of aqueous parenteral formulation, as well as in altering the oral bioavailability. According to the Lipinski's rule, drugs with octanol/water partition coefficient (log P) <5.0 possess more drug-likeness than the compounds with larger log P values (24). We report that the log P value of EFAH in octanol/water system is 0.33.

When compound **4** was labelled with Tc-99m in the presence of tricine and stannous chloride, over 98% of labelling yield was obtained. Because of the ideal nuclear characteristics, Tc-99m ($T_{1/2}$ = 6 h, 140 KeV) remains the most commonly used radionuclide for SPECT. It easily forms a stable complex with hydrazinonicotinamide. The labelled compound **5** was characterized by HPLC (Figure 2). The retention time of Tc-99m-labelled EFAH was measured as 9.25 min. When challenged with human plasma, there was negligible decomplexation of Tc-99m radioactivity for up to 24 h of incubation (Figure 2).

In vitro *anticancer activity of EFAH*

A significant concern in modifying drugs for radiolabelling purposes is the tendency of modified drug to lose activity and/or potency. Therefore, we evaluated EFAH in multiple cells lines and compared its antiproliferative activity with that of EF24. The experimental data demonstrated that EFAH was as effective as EF24 in H441, Panc-1 and MiaPaCa-2 cell lines. Cell proliferation was studied in cancer cells in culture by estimating the decrease in the activity of lysosomal enzyme hexosaminidase (Figure 3). It is clear that EFAH possessed significant antiproliferative activity in all the three cells tested, and the potency was comparable with that shown by EF24. The results suggest that EFAH can be further developed as an imageable anticancer compound.

Biodistribution and imaging of Tc-99m-EFAH

The importance of imaging in cancer drug development is increasing with advances in instrumentation, chemistry and imaging technologies (25). The objective behind this strategy has been to enable monitoring of the adequacy and selectivity of drug accumulation in pathologic tissue. A textbook example may be the pretherapy elucidation of ibritumomab distribution by imaging before initiating radioimmunotherapy of non-Hodgkin's lymphoma with Y-90-labelled ibritumomab or Zevalin (26). In the presented work, we report a similar approach to the development of synthetic curcuminoids.

We followed up our *in vitro* study by investigating *in vivo* biodisposition of Tc-99m-EFAH in a rat model of xenograft lung tumour. Figure 4 shows the accumulation of radioactivity in various organs after 24 h of injection. The accompanying whole-body images are shown in Figure 5, and they confirm the overall results obtained from biodistribution data. In the sequential images through 24 h, the radiolabelled compound appeared to travel from liver to intestine and into the faeces. No other organ except liver and intestines accumulated significant radioactivity, suggesting that its clearance depended on hepatobiliary route.

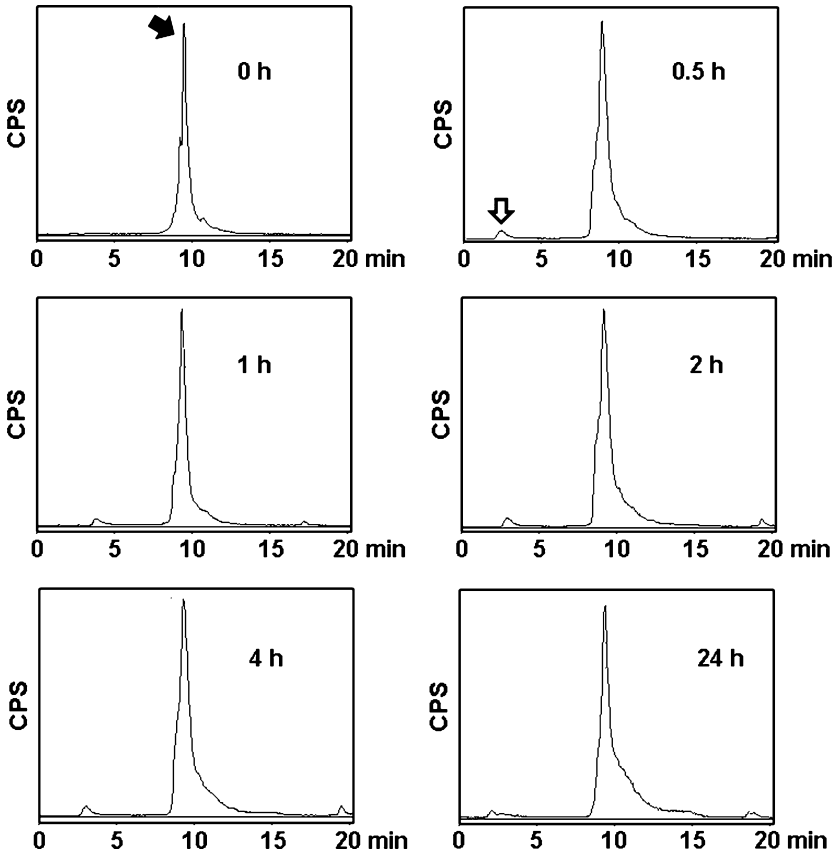

Figure 2: The stability of Tc-99m-EFAH was analysed by reverse-phase radioHPLC using a 20-min acetonitrile gradient (20–100%). The labelled compound was incubated with human plasma at 37 °C, and the appearance of free Tc-99m-pertechnetate peak at 2.5–2.75 min (white arrow) was monitored over time. Labelled compound eluted at just <10 min (black arrow).

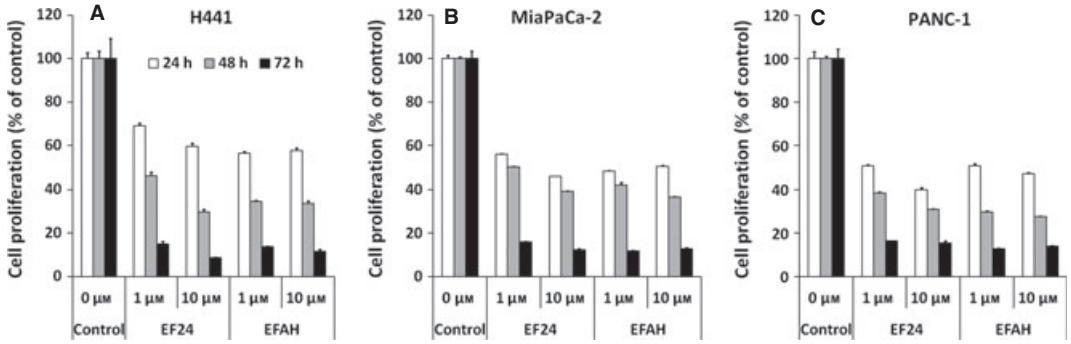

Figure 3: EFAH inhibits proliferation of (A) lung adenocarcinoma H441 cells, and pancreatic cancer cells (B) MiaPaCa-2 and (C) Panc-1. The cells were treated with 1 and 10 μM EFAH for 24–72 h, and the cell proliferation was measured by estimating hexosaminidase activity as described in the text.

As expected, the tumour tissue accumulated measurable, but little radiolabelled compound. The same observation was made in the scintigraphic images. Previously, Ravindranath and Chandrasekhara (27) reported that the majority of tritiated (H-3) curcumin administered in rats eliminated in faeces. The *in vivo* behaviour of Tc-99m-EFAH is suggestive of a stable complex of Tc-99m. When the rat urine collected after 30 min of injection was injected in HPLC column, no free Tc-99m radioactivity was found (data not shown).

Efficacy of EFAH as an antiproliferative agent

To test whether EFAH is active as an antiproliferative agent *in vivo*, we administered EFAH in a mouse model of xenograft Panc-1 tumours. The xenograft tumours were allowed to grow to a size of approximately 500 mm^3, following which EFAH was intraperitoneally administered on daily basis for 3 weeks. We observed a remarkable reduction in tumour size after treatment with EFAH. EFAH inhibited the growth of the tumours xenografts (Figure 6), whereas the control tumours grew during the treat-

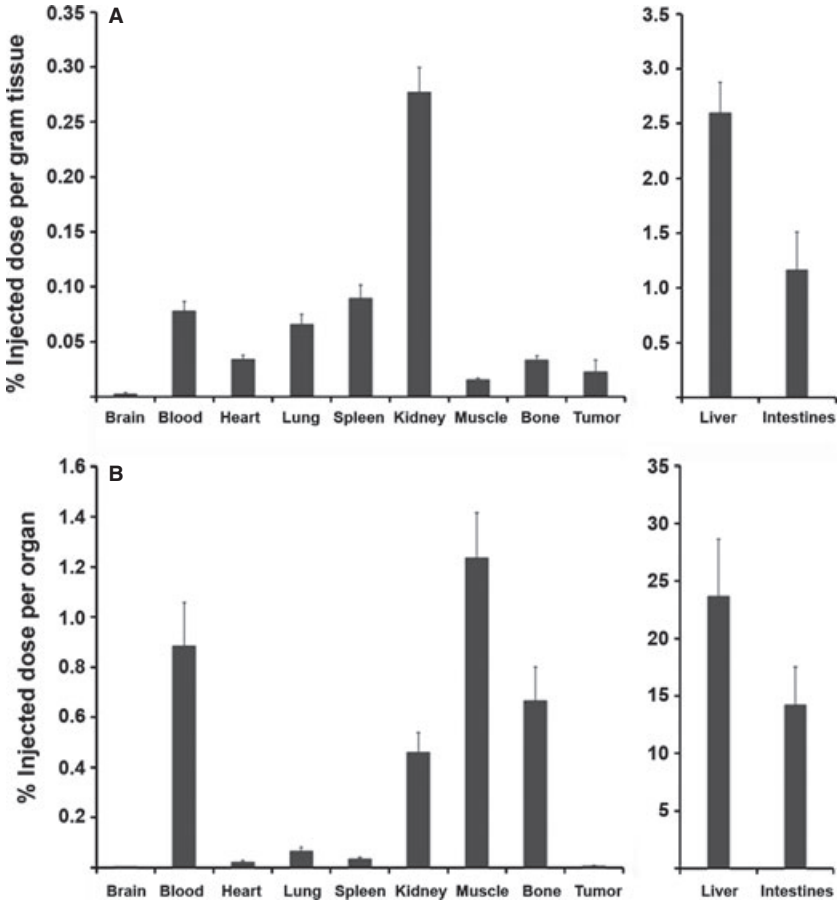

Figure 4: Biodistribution of Tc-99m-EFAH in nude rats carrying H441 xenograft tumours. (A) Per cent injected dose per gram of tissue and (B) per cent injected dose per organ. The rats were intravenously injected with about 500 μCi of Tc-99m-EFAH and euthanized after 24 h for biodistribution.

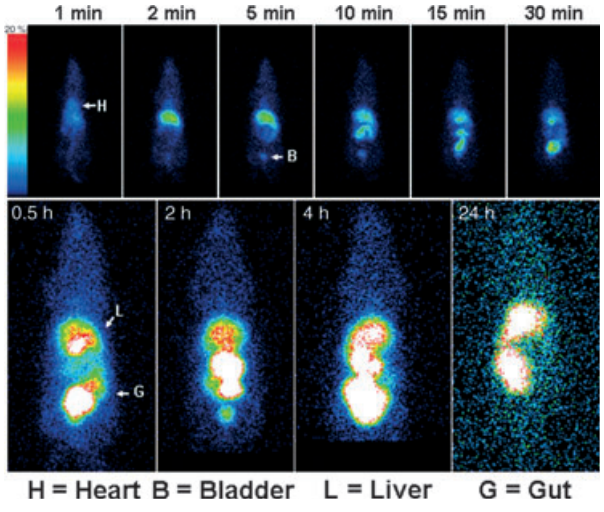

Figure 5: Gamma camera images of rats injected with Tc-99m-EFAH: rats injected with approximately 500 μCi of Tc-99m-EFAH were imaged in a NanoSPECT system. A dynamic image acquisition of Tc-99m-EFAH kinetics in the first 30 min of intravenous administration (upper panel) was followed by static images (at 0.5, 2, 4 and 24 h) showing accumulation of Tc-99m-EFAH in liver and gut.

ment period, reaching a size of over 2000 mm^3. Panc-1 tumours in the EFAH-treated animals were smaller throughout, measuring approximately 434 mm^3 at the end of the treatment period. The excised tumours from the EFAH-treated mice averaged 0.45 g, whereas those from the control group weighed about 2.5 g (Figure 6B).

Although the mechanism of action of EF24 is not clearly understood, evidences suggest that it causes apoptosis via a redox-dependent mechanism (28,29). EF24 and its analogues containing dienone moiety are capable of serving as Michael acceptors. In cisplatin-resistant ovarian cancer cells, EF24 was found to cause apoptotic cell death by induction of PTEN and inhibition of AKT activities (30). In a more elaborate *in vivo* study by Subramaniam, *et al.*, (15) EF24 was found to induce caspase-mediated apoptosis in HCT-116 colon cancer xenografts. At the same time, marked reduction in AKT activity, as well as decreased cyclooxygenase-2, interleukin-8, and vascular endothelial growth factor mRNA, and protein expression was reported (15). All these studies show that EF24-induced apoptosis is accompanied by G2-M cell cycle arrest. Further, EF24 has been shown to suppress NF-kB signalling pathway through a direct action on IκB kinase in lung, breast, ovarian and cervical cancer cells (31). NF-kB plays an important role in oncogenesis, and there is significant evidence to hypothesize that the anticancer activity of curcuminoids may be mediated by inhibition of NF-kB

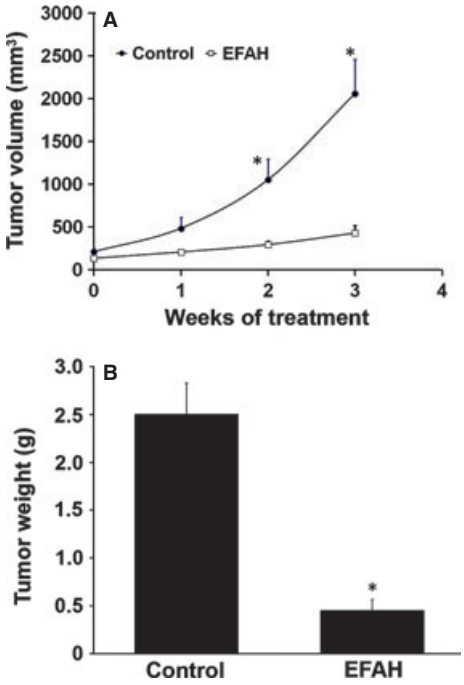

Figure 6: Treatment of nude mice ($n = 4$ per group) carrying xenograft Panc-1 tumours with EFAH inhibits the growth of tumours-(A) tumour volume and (B) tumour weight at necropsy. The mice were intraperitoneally injected with 5 μg of EFAH on daily basis for 3 weeks. Asterisk (*) is $p < 0.05$ compared to untreated control.

activity (32). Further mechanistic studies may be needed for complete understanding of the specific signalling pathways responsible for the tumour-suppressive properties of EFAH and EF24 in pancreatic cancer.

Conclusions and Future Directions

Anticancer therapy combined with image-derived knowledge of drug accumulation enables more realistic and effective treatment planning, and may be of benefit in predicating tumour response as well as timely change of therapeutic course. We synthesized a derivative of curcuminoid EF24 amenable to radiolabelling with Tc-99m. The derivative was tested in various cancer lines to ensure that the anticancer activity of EF24 is not compromised by chemical modification. We have previously shown that the putative pharmacophore of EF24 is the enone portion (23). Because this pharmacophore is preserved in EFAH, we speculate that EFAH retains the same mechanism of action. Nevertheless, it needs to be proven by empirical data which is beyond the scope of this study. The biodistribution and imaging results suggest that because of the natural clearance into the intestine, EFAH might have an added advantage in the treatment for colon cancer. The application of oral delivery and the use of EFAH in a mouse model of colon cancer are the subjects of another investigation being pursued in our laboratory.

Acknowledgments

The authors are thankful to the OUHSC-Nuclear Pharmacy for supplying Tc-99m-pertechnetate radioactivity. The authors also acknowledge the funding from National Cancer Institute (R03 CA143614-01).

References

1. Altar C.A. (2008) The Biomarkers Consortium: on the critical path of drug discovery. Clin Pharmacol Ther;83:361–364.
2. Altar C.A., Amakye D., Bounos D., Bloom J., Clack G., Dean R., Devanarayan V. *et al.* (2008) A prototypical process for creating evidentiary standards for biomarkers and diagnostics. Clin Pharmacol Ther;83:368–371.
3. Woodcock J., Woosley R. (2008) The FDA critical path initiative and its influence on new drug development. Annu Rev Med;59:1–12.
4. Pomper M.G. (2002) Can small animal imaging accelerate drug development? J Cell Biochem Suppl;39:211–220.
5. Aggarwal B.B., Shishodia S. (2006) Molecular targets of dietary agents for prevention and therapy of cancer. Biochem Pharmacol;71:1397–1421.
6. Aggarwal S., Ichikawa H., Takada Y., Sandur S.K., Shishodia S., Aggarwal B.B. (2006) Curcumin (diferuloylmethane) down-regulates expression of cell proliferation and antiapoptotic and metastatic gene products through suppression of IkappaBalpha kinase and Akt activation. Mol Pharmacol;69:195–206.
7. Aggarwal B.B., Shishodia S. (2004) Suppression of the nuclear factor-kappaB activation pathway by spice-derived phytochemicals: reasoning for seasoning. Ann N Y Acad Sci;1030:434–441.
8. Aggarwal B.B., Takada Y., Oommen O.V. (2004) From chemoprevention to chemotherapy: common targets and common goals. Expert Opin Investig Drugs;13:1327–1338.
9. Anto R.J., Mukhopadhyay A., Denning K., Aggarwal B.B. (2002) Curcumin (diferuloylmethane) induces apoptosis through activation of caspase-8, BID cleavage and cytochrome c release: its suppression by ectopic expression of Bcl-2 and Bcl-xl. Carcinogenesis;23:143–150.
10. Anand P., Kunnumakkara A.B., Newman R.A., Aggarwal B.B. (2007) Bioavailability of curcumin: problems and promises. Mol Pharm;4:807–818.
11. Ravindranath V., Chandrasekhara N. (1980) Absorption and tissue distribution of curcumin in rats. Toxicology;16:259–265.
12. Pati H.N., Das U., Quail J.W., Kawase M., Sakagami H., Dimmock J.R. (2008) Cytotoxic 3,5-bis(benzylidene)piperidin-4-ones and *N*-acyl analogs displaying selective toxicity for malignant cells. Eur J Med Chem;43:1–7.
13. Robinson T.P., Hubbard R.B.t., Ehlers T.J., Arbiser J.L., Goldsmith D.J., Bowen J.P. (2005) Synthesis and biological evaluation of aromatic enones related to curcumin. Bioorg Med Chem;13:4007–4013.
14. Sun A., Shoji M., Lu Y.J., Liotta D.C., Snyder J.P. (2006) Synthesis of EF24-tripeptide chloromethyl ketone: a novel curcumin-related anticancer drug delivery system. J Med Chem;49:3153–3158.
15. Subramaniam D., May R., Sureban S.M., Lee K.B., George R., Kuppusamy P., Ramanujam R.P., Hideg K., Dieckgraefe B.K., Hou-

chen C.W., Anant S. (2008) Diphenyl difluoroketone: a curcumin derivative with potent in vivo anticancer activity. Cancer Res;68:1962–1969.
16. Abrams M.J., Juweid M., tenKate C.I., Schwartz D.A., Hauser M.M., Gaul F.E., Fuccello A.J., Rubin R.H., Strauss H.W., Fischman A.J. (1990) Technetium-99m-human polyclonal IgG radiolabeled via the hydrazino nicotinamide derivative for imaging focal sites of infection in rats. J Nucl Med;31:2022–2028.
17. Landegren U. (1984) Measurement of cell numbers by means of the endogenous enzyme hexosaminidase. Applications to detection of lymphokines and cell surface antigens. J Immunol Methods;67:379–388.
18. Ravindran J., Prasad S., Aggarwal B.B. (2009) Curcumin and cancer cells: how many ways can curry kill tumor cells selectively? AAPS J;11:495–510.
19. Sahoo K., Dozmorov M.G., Anant S., Awasthi V. (2010) The curcuminoid CLEFMA selectively induces cell death in H441 lung adenocarcinoma cells via oxidative stress. Invest New Drugs; In Press: doi: 10.1007/s10637-010-9610-4 (Epub ahead of print).
20. Agashe H., Sahoo K., Lagisetty P., Awasthi V. (2011) Cyclodextrin-mediated entrapment of curcuminoid 4-[3,5-bis(2-chlorobenzylidene-4-oxo-piperidine-1-yl)-4-oxo-2-butenoic acid] or CLEFMA in liposomes for treatment of xenograft lung tumor in rats. Colloids Surf B Biointerfaces;84:329–337.
21. Adams B.K., Ferstl E.M., Davis M.C., Herold M., Kurtkaya S., Camalier R.F., Hollingshead M.G., Kaur G., Sausville E.A., Rickles F.R., Snyder J.P., Liotta D.C., Shoji M. (2004) Synthesis and biological evaluation of novel curcumin analogs as anti-cancer and anti-angiogenesis agents. Bioorg Med Chem;12:3871–3883.
22. Lagisetty P., Powell D.R., Awasthi V. (2009) Synthesis and structural determination of 3,5-bis(2-fluorobenzylidene)-4-piperidone analogs of curcumin. J Mol Struct;936:23–28.
23. Lagisetty P., Vilekar P., Sahoo K., Anant S., Awasthi V. (2010) CLEFMA – an anti-proliferative curcuminoid from structure activity relationship studies on 3,5-bis(benzylidene)-4-piperidones. Bioorg Med Chem;18:6109–6120.
24. Lipinski C.A., Lombardo F., Dominy B.W., Feeney P.J. (2001) Experimental and computational approaches to estimate solubility and permeability in drug discovery and development settings. Adv Drug Deliv Rev;46:3–26.
25. Griffiths G.L. (2008) The imaging probe development center and the production of molecular imaging probes. Curr Chem Genomics;1:65–69.
26. Iagaru A., Gambhir S.S., Goris M.L. (2008) 90Y-ibritumomab therapy in refractory non-Hodgkin's lymphoma: observations from 111In-ibritumomab pretreatment imaging. J Nucl Med;49:1809–1812.
27. Ravindranath V., Chandrasekhara N. (1981) Metabolism of curcumin – studies with [3H]curcumin. Toxicology;22:337–344.
28. Adams B.K., Cai J., Armstrong J., Herold M., Lu Y.J., Sun A., Snyder J.P., Liotta D.C., Jones D.P., Shoji M. (2005) EF24, a novel synthetic curcumin analog, induces apoptosis in cancer cells via a redox-dependent mechanism. Anticancer Drugs;16:263–275.
29. Sun A., Lu Y.J., Hu H., Shoji M., Liotta D.C., Snyder J.P. (2009) Curcumin analog cytotoxicity against breast cancer cells: exploitation of a redox-dependent mechanism. Bioorg Med Chem Lett;19:6627–6631.
30. Selvendiran K., Tong L., Vishwanath S., Bratasz A., Trigg N.J., Kutala V.K., Hideg K., Kuppusamy P. (2007) EF24 induces G2/M arrest and apoptosis in cisplatin-resistant human ovarian cancer cells by increasing PTEN expression. J Biol Chem;282:28609–28618.
31. Kasinski A.L., Du Y., Thomas S.L., Zhao J., Sun S.Y., Khuri F.R., Wang C.Y., Shoji M., Sun A., Snyder J.P., Liotta D., Fu H. (2008) Inhibition of IkappaB kinase-nuclear factor-kappaB signaling pathway by 3,5-bis(2-flurobenzylidene)piperidin-4-one (EF24), a novel monoketone analog of curcumin. Mol Pharmacol;74:654–661.
32. Rayet B., Gelinas C. (1999) Aberrant rel/nfkb genes and activity in human cancer. Oncogene;18:6938–6947.

Supporting Information

Additional Supporting Information may be found in the online version of this article:

Appendix S1. NMR and mass spectroscopy data.

Please note: Wiley-Blackwell is not responsible for the content or functionality of any supporting materials supplied by the authors. Any queries (other than missing material) should be directed to the corresponding author for the article.M